Edge effects on phonon dispersion and density-of-states of graphene nanoribbons and nanoflakes

F. Mazzamuto,[1,*] A. Valentin,[1,†] C. Chassat,[1] J. Saint-Martin,[1] and P. Dollfus[1]

[1] *Institut d'Electronique Fondamentale, Univ. Paris-Sud, CNRS, UMR 8622, F-91405 Orsay, France*

(Received April 12, 2010)

We calculate the phonon dispersion and the vibrational density of states (VDOS) of semi-infinite GNRs and nanoflakes of various width and edge orientations using the force constant model including fifth-nearest neighbour atoms. Besides typical graphene peaks like E2g (G peak) and D, we clearly identify several distinctive ribbon peaks in ribbon VDOS depending on the edge shape. In particular, most of armchair modes have been detected at about 1350 cm^{-1} and 1480 cm^{-1}, associated with strong localized in-plane vibrations, and at about 630 cm^{-1}, associated with out-of plane vibrations. VDOS is also calculated for graphene nanoflakes to identify the minimal GNR length for which typical armchair and zigzag peaks can be observed. Typical localized modes appear for ribbon longer than 10 nm. Therefore, the edge nature can be identified by detecting the characteristic ribbon peaks in the VDOS.

PACS numbers: 63.22.Rc

I. INTRODUCTION

Carbon-based nanomaterials have been intensely investigated in the past decade, and today, great attention is focused on graphene nanoribbons (GNRs), especially for their structure-dependent phonons and electronic properties [1, 2]. These nanostructures are expected to open a large field in nanoelectronics [3–5], spintronics [6, 7] and thermoelectric applications [8]. The predicted giant thermoelectric coefficient [9] as well as the strong electron-phonon coupling [10] have recently oriented many works on the study of GNR vibration dynamics. Raman spectroscopy has been widely used to investigate graphite [9, 11, 12] and single or multilayer graphene sheets [13] and recently for semi-infinite graphene edges [14] and GNRs [15, 16]. Theoretical calculations on the basis of density-functional theory [17], empirical bond order potential energy [1, 18], or valence force field model [9, 19, 20] have supported experimental results but lots of questions are still open. The D peak detected in Raman spectra of all graphene-based structures is one of the most controversial points debated in last decade [10, 21, 22]. Associated with the breathing modes of sp2 atoms in rings [9], the D peak has been studied as function of the number of graphene layers [13] and recently, the crystalline disorder dependence has been considered [23]. In this sense, armchair edges act as crystalline defects and could be responsible for the high intensity D peak detected at 1350 cm^{-1} in Raman spectra of graphene edges [10]. Additionally, around the G peak, the presence of the doubly degenerate zone center E2g mode [15] yields also some open questions. The results of recent calculations on the basis

of the density-functional theory [11] are sensibly shifted from experimental data [24, 25].

As successfully done for nanotubes [23], we study here the phonon dispersion and the vibrational density of state (VDOS) of semi-infinite GNRs and graphene nanoflakes (GNFs) on the basis of calculations performed within the empirical force-constant model (FCM). The VDOS has been carefully examined to distinguish the specific vibration modes associated with armchair-GNRs (AGNRs) or zigzag-GNRs (ZGNRs) and to study the behavior of these modes when length limits are introduced. An interesting way to distinguish AGNR and ZGNR and to assess the GNR edge quality is proposed by the analysis of specific peak intensities in VDOS. A similar experimental method has been recently suggested. It basically involves the detection of characteristic peaks in the Raman spectrum of GNRs or semi-infinite graphene edges [26–29]. By comparing relevant vibration modes in calculated VDOS to Raman spectrum peaks, lots of correspondences have been found to validate the model and new characteristic modes are predicted. Finally, particular armchair and zigzag vibrational modes are analyzed in zero-dimensional structure (GNFs) to understand the effect of length in finite ribbons.

The paper is organized as follows: we first introduce the model and the methodology to calculate the phonon dispersion and VDOS. Then VDOS for perfect AGNR and ZGNR are presented and discussed. Finally, the VDOS of GNFs is compared to that of semi-infinite GNR.

II. MODEL AND METHODOLOGY

Phonon dispersions and density of state are investigated for semi-infinite AGNR, ZGNR and GNF by means of numerical calculation based on the empirical force-constant (FC) model. Starting from a two-dimensional (2D) graphene sheet, boundary conditions are introduced and the one-dimensional (1D) or zero-dimensional unit cell in reciprocal space is treated (see Figs. 1(a) and 1(b) for illustration). In particular, we perform the Fourier transform of the classical motion equation

$$m_i \, \ddot{\vec{u}}_i = \sum_j K^{(ij)} \left(\vec{u}_j - \vec{u}_i \right) \ , \quad (i = 1, \ldots, N) \, , \tag{1}$$

where $\vec{u}_i = (x_i, y_i, z_i)$ and m_i are the displacement and the mass of the i-th atom, respectively, in the N atom unit cell. $K^{(ij)}$ stands for the force-constant tensor that couples the i-th and j-th atoms. The sum over j in Eq. (1) is taken over the neighbors of the i-th atom. The relevant rank of neighbors considered in graphene lattice has been gradually enhanced up to the fifth-nearest-neighbor until a satisfactory agreement with experimental results was reached. Here the fifth nearest neighbor model is used with force constant parameters determined by Mohr [30]. It has been shown that the coupling between in-plane and out-of-plane atom displacements can be neglected [31], and the possible presence of substrate does not affect sensibly the single graphene sheet phonon dispersion if the coupling is Van der Waals force type, like inter-plane forces in graphite. Calculation is thus simplified by considering uncoupled in-plane and out-of plane motion equations and neglecting the substrate

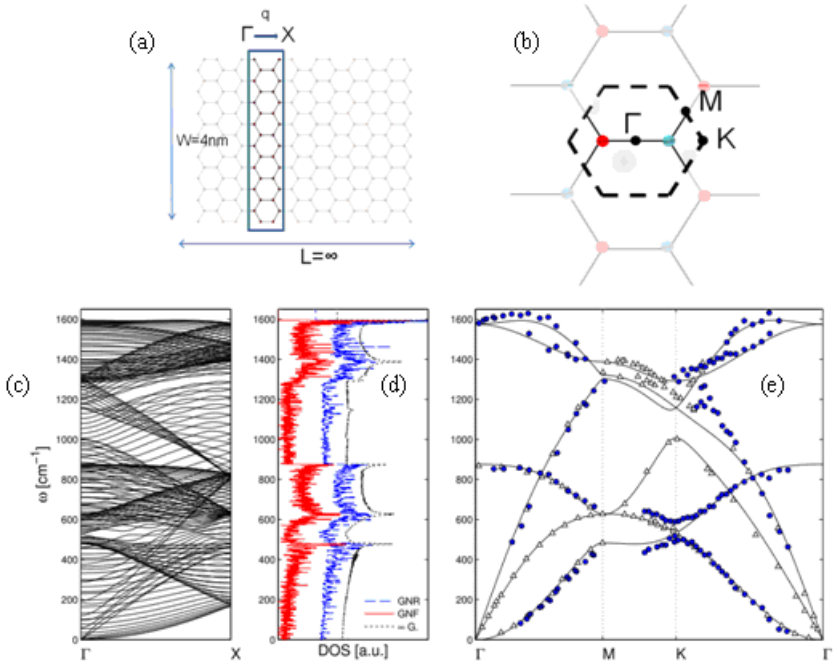

FIG. 1: (a) Periodical lattice scheme of an AGNR and (b) graphene sheet elementary cell. (c) Phonon dispersion of a perfect 32-AGNR. (d) VDOS of the 4 nm×20 nm GNF, 4 nm AGNR and 2D graphene. (e) Calculated phonon dispersion in graphene (lines) and some experimental results (symbols) [32].

effect. The solutions take the form of frequency and amplitude of each single-ion vibration mode in the three space directions as a function of the wave vector. The phonon dispersion for an AGNR of a width of about 4 nm and infinite length is shown in Fig. 1(b). Besides, the phonon dispersion calculated for 2D single graphene sheet (lines) is compared in Fig. 1(d) to experimental data [9], which illustrates the accuracy of the model according to the position in k-space. A good match is obtained in almost the full space except for the zone around the K point. Indeed, the FC model gives only an empirical description of atomic vibrations while neglecting the electron-phonon coupling demonstrated to be significant at this point. Therefore, the discrepancies between calculated and experimental results are not surprising near K point, especially for high-energy modes.

The phonon DOS can be easily extracted from the phonon dispersion via an appropriate reciprocal-space discretization. As examples, the DOS of 4 nm AGNR (32-AGNR), 4 nm×20 nm GNF and 2D graphene are shown in Fig. 1(d).

Ribbons are defined by their approximate width W calculated as the distance of the outmost dimmers (refer to Fig. 1(a)) or more precisely by the number of dimmers M in the unit cell. The relationships between width and M are given by

$$W_{AGNR} = \frac{1}{2}\,(M-1)\,a_0 \tag{2}$$

and

$$W_{ZGNR} = \frac{\sqrt{3}}{2}\,(M-1)\,a_0, \tag{3}$$

where a_0 is the lattice constant. It was shown in ref. [14] that the average bond length in a GNR rapidly converges to the average bond length of a relaxed sheet of graphene on increasing the atom number. In our calculation, the atom bond length has been approximated as the bond length of relaxed sheet of graphene. GNR relaxation is thus neglected and the lattice constant of relaxed graphene sheet, i.e., $a_0 = 2.4656$ Å, is used.

To identify the contribution of edge-localized modes and typical 2D graphene modes, the local vibrational density of states (LVDOS) is calculated at each single atomic site i as

$$\rho_i(\omega) = \int_{\Gamma}^{\mathrm{X}} \sum_{p=1}^{3N} \left| \overrightarrow{U}_i^p(q) \right|^2 \delta\left(\omega - \omega_p\right) dq\,, \tag{4}$$

where $\overrightarrow{U}_n^p\,(q)$ is the three-dimensional (3D) vector describing the vibration of the i-th ion for the mode p as a function of the wave vector q. The $3N$ vibrational modes associated with the 3D displacement of the N ions in the unit cell are considered. Two types of LVDOS are considered throughout the paper: (i) edge LVDOS, obtained as the sum of all DOS associated with edge atoms; (ii) central LVDOS obtained as the sum of all DOS associated with inner ribbon atoms. The two separated zones are shown in Fig. 2 for both AGNR and ZGNR.

The method is finally applied to graphene ribbons of finite length and width, i.e., nanoflakes. In this case, structures are zero-dimensional, and no lattice periodical condition can be used to simplify the dynamical matrix. Vibrational modes are thus directly calculated by solving Eq. (1) for the whole structure and the LVDOS is extracted by summing all modes detected at a specific frequency, i.e.,

$$\rho_i(\omega) = \sum_{p=1}^{3N} \left| \overrightarrow{U}_i^p \right|^2 \delta\left(\omega - \omega_p\right), \tag{5}$$

where the displacement vector $\overrightarrow{U}_n^p$ is no longer wave vector-dependent.

III. RESULTS

We investigate, in this section, the impact of ribbon-edge type on VDOS. The importance of edge boundary condition on vibrational dynamics is considered at first by comparing the VDOS of an infinite 2D graphene sheet with that of GNRs. The total GNR VDOS is divided into two components displayed separately in Fig. 2(a) and 2(b) for AGNR and ZGNR, respectively. The first component is associated with vibrations of inside atoms, and hence not affected by edge vibrations. The second one is associated with edge-atom vibrations. The two separated areas of the ribbon are illustrated in insets of Fig. 2.

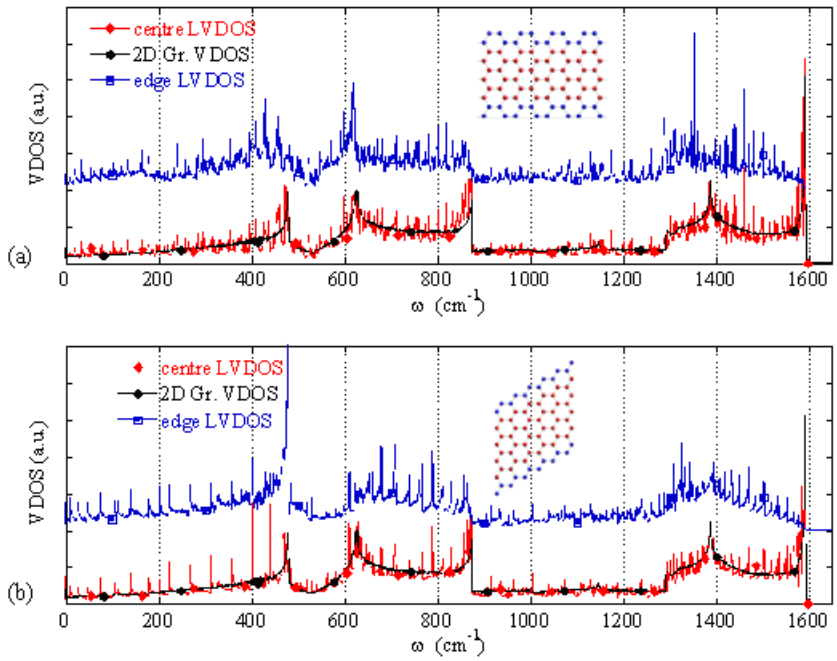

FIG. 2: Edge LVDOS (blue) and central LVDOS (red) of (a) 32-AGNR and (b) 32-ZGNR superimposed on 2D graphene VDOS (black).

III-1. Vibration modes of AGNR

A perfect and semi-infinite AGNR has been analyzed at first. The LVDOS of inner atoms are superimposed on 2D graphene sheet VDOS in Fig. 2(a). As expected, vibrational dynamics inside the ribbon are similar to vibrational modes in 2D graphene, and typical graphene modes can be clearly identified. The notorious graphene E_{2g} and D peaks detected in Raman spectra at about 1350 cm^{-1} and 1580 cm^{-1} are found in calculated center LVDOS at about 1380 cm^{-1} and 1590 cm^{-1}, respectively. This small frequency mismatch is probably due to the model limitation at K point, as discussed in Section II. Vibrational dynamics inside the ribbon are similar to that of 2D graphene, especially for GNR larger than a few nanometers, where the effect of boundary condition can be mainly neglected. This effect cannot be neglected for frequencies close to 1460 cm^{-1}, where an intense peak can be observed in the center LVDOS of the ribbon, while it is not seen in the DOS of 2D graphene. When analyzing the vibrational modes detected at $\approx$ 1460 cm^{-1}, we find that this peak is associated with strong atom vibrations localized in the center of the ribbon or in symmetrical atom substripes with edge atoms completely frozen. An example of such vibrational mode detected at these frequencies is presented in Fig. 3(a). These phonon modes are specific to AGNR; as seen in Fig. 2(b), the peak at $\approx$ 1460 cm^{-1} is not detected in the central LVDOS of ZGNR.

In a recent work [13], the Raman spectrum of GNRs has been investigated and some peaks different from that of 2D graphene spectrum have been detected. Correspondence

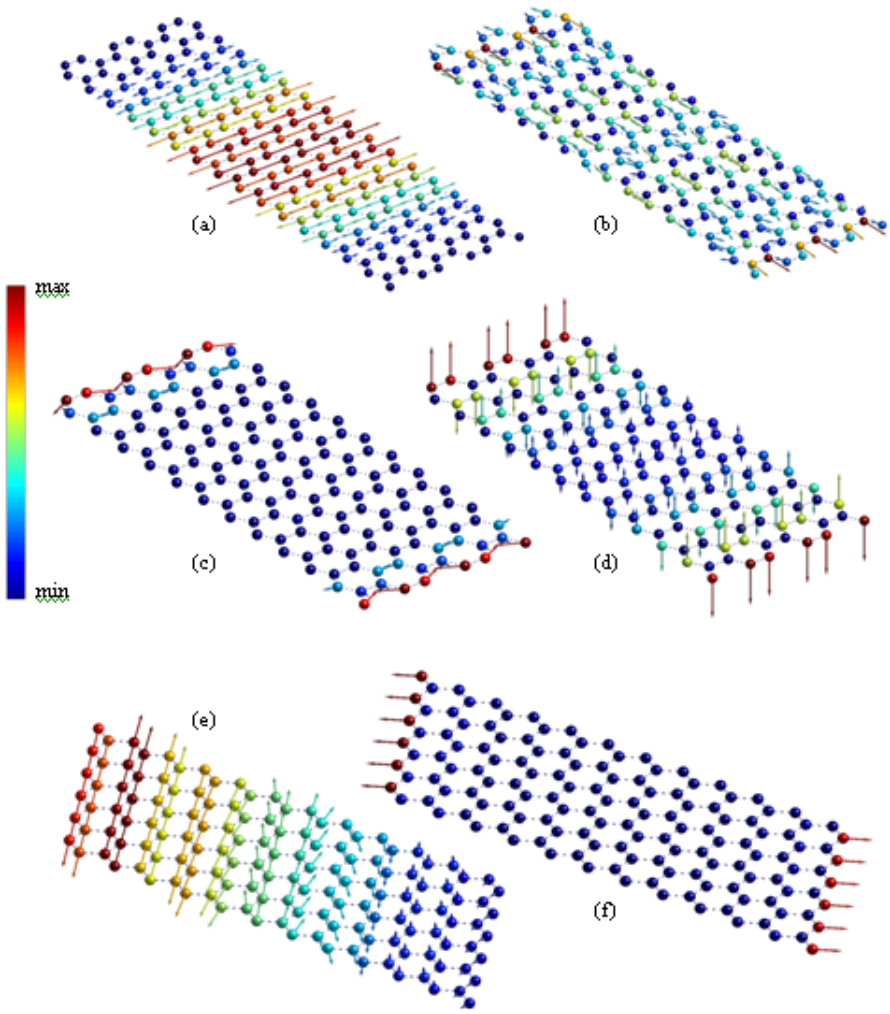

FIG. 3: Illustration of some vibration modes in GNRs: (a) Central mode in 32-AGNR at 1460 cm^{-1}; (b) Edge mode in 32-AGNR at 1460 cm^{-1}; (c) Edge mode in 32-AGNR at 1350 cm^{-1}; Out-of-plane edge mode in 32-AGNR at 630 cm^{-1}; (d,e) Edge modes in 32-ZGNR at 480 cm^{-1}.

between Raman spectrum peaks with that calculated in VDOS can be considered here. In experimental spectra, a peak at similar frequency ($\approx$ 1450 cm^{-1}), which is strongly dependent on the width and edge structure, has been detected. It is remarkable to see in Fig. 2(a) that this peak appears in both center LVDOS (red) and edge LVDOS (blue) of AGNR. As expected, on increasing the width of the ribbon, the impact of specific modes decreases and the total VDOS tends to the VDOS of 2D graphene (not shown). To explain the edge dependence of the peaks, let us focus on edge-atom vibrations. The peak observed in edge LVDOS of 32-AGNR (Fig. 2(a), blue) at 1460 cm^{-1} is associated with vibration of the second or third outmost dimmers (as illustrated in Fig. 3(b)), and the origin of

these edge modes is again the armchair nature of the ribbon edges. There is no equivalent peak in the LVDOS of ZGNR. In summary, the peak observed at 1460 cm^{-1} can be really considered as an armchair signature in the VDOS of a GNR. At this frequency, a high density of phonons is strongly localized at the edges or in substripes inside the ribbon.

Another interesting point in the VDOS is the peak centered on about 1350 cm^{-1}, i.e. on the same frequency as the D peak in Raman spectra. This Raman D peak has been considered in a recent work on Raman spectroscopy as an indicator of armchair edges. Looking at the edge LVDOS of AGNR in Fig. 2(a), a strong peak can be distinguished at this frequency. The corresponding modes are associated with strong vibrations of outmost dimmers. An example of these modes is presented in Fig. 3(c): this optic-like edge-atom motion is a consequence of the central symmetry of the armchair elementary cell. This is another signature of AGNR.

Thus far, all the considered modes are vibration parallel to the ribbon surface (in-plane-vibration). To complete the analysis on AGNR, the out-of-plane vibrations are accessed. It should be noted that only the sum of out-of-plane and in-plane modes is shown in Fig. 2, but they are considered separately; it can be easily identified that the peak at 630 cm^{-1} is exclusively due to out-of-plane vibration in AGNR. The corresponding modes are associated with edge oscillations leading to a twisting of the ribbon, as illustrated in the example of mode representation shown in Fig. 3(c).

III-2. Vibration modes of ZGNR

Attention is now focused on ZGNRs. A similar analysis for in/out-of-plane and edge or center localized vibrations can be done. There is no significant peak in out-of-plane VDOS; hence, the study is oriented towards in-plane modes. Edge and center LVDOS of the 32-ZGNR is presented in Fig. 2(b) and the two separated areas are illustrated in the inset. As done for AGNR, the center LVDOS was compared to VDOS of 2D graphene. Two main ZGNR peaks at low frequencies can be distinguished when comparing the two VDOS. These two peaks are associated with vibrational modes strongly localized in the ribbon center. The zigzag edge orientation is certainly responsible for these modes because no such low-energy peaks is visible in the AGNR center LVDOS. However, the main remarkable zigzag peaks can be distinguished in the edge LVDOS reported in Fig. 2(b): the peak detected at about 480 cm^{-1} is associated with in-plane displacements of the atoms localized at the edge of the ribbon. In Fig. 3, examples of longitudinal edge mode (e) and breathing-like vibration (f) detected at this frequency are shown. This is a clear signature of ZGNR.

III-3. Vibration modes of GNFs

Attention is now focused on vibrational dynamics of GNF with aim of understanding how the length limit can affect the VDOS and the specific modes observed in zigzag and armchair ribbons. Thus far, we calculated the LVDOS for a 32-AGNR with length boundary condition. In other words, the LVDOS is calculated for GNFs of the same width as the GNR studied previously but for different finite lengths. GNF structures, shown in insets of Fig. 4, have been built as finite sequences of the elementary cell with armchair edges

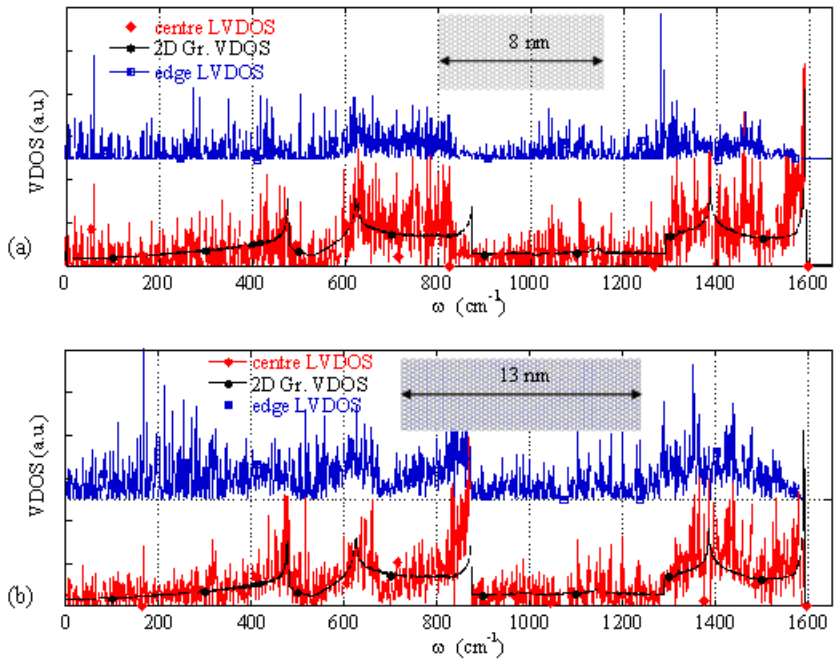

FIG. 4: Edge LVDOS (blue) and central LVDOS (red) of (a) a 4 nm×8 nm GNF and (b) a 4 nm×13 nm GNF superimposed on the VDOS of 2D graphene (black).

that are used to treat infinite the 32-AGNR. It should be noted that the analyzed GNFs have a rectangular shape with top-bottom edges different from the lateral ones. Hence, the edge LVDOS can be affected by both armchair and zigzag typical vibrations. We present here the results obtained for two GNFs with bottom/up armchair edges longer than lateral zigzag edges, i.e., a 4 nm×8 nm GNF and a 4 nm×13 nm GNF, which correspond to a sequence of 20 and 30 elementary cells, respectively.

In Fig. 4, we plot the calculated VDOS of GNFs divided in center and edge-localized vibration. Central LVDOS is superimposed on 2D graphene VDOS. First of all, it should be noted that for very small GNF with a length of few nanometers, the specific GNR modes cannot be indentified (not shown). The specific armchair peaks at 1380 cm^{-1} and 1460 cm^{-1} become visible for the GNF of Fig. 4(a) (4 nm×8 nm). However, these peaks are not dominant and their intensity is weaker than in the case of GNR. The intensity of these peaks is related to finite length boundary condition and to the mixing of armchair and zigzag edges, which spreads the peaks over other frequencies. Actually, on increasing the GNF length, the specific armchair peaks appear more clearly, as in the case of the second GNF presented in Fig. 4(b), i.e., the 4 nm×13 nm GNF. The VDOS is weakly affected by the finite length and very similar to that of the GNR. In summary, we can generally conclude that the finite length does not affect the vibrational dynamics of GNR if the ribbon is longer than about 10 nm. For a shorter ribbon, or more precisely for smaller nanoflakes, specific armchair peaks rapidly reduce until they fully disappear for a GNF length of a few

nanometers.

IV. CONCLUSION

The empirical Force-Constant Model including interactions with the fifth nearest neighbor atoms has been successfully used to study the vibrational properties of GNRs and GNFs. The calculation was shown to give an overall good description of the phonon modes in these graphene nanostructures. The detailed analysis of the local VDOS has allowed us to identify some specific AGNR and ZGNR peaks strongly related to the edge-ribbon structure. Hence, the nature of the ribbon edges can be identified by investigating the structure-dependent local VDOS. Additionally, the analysis of GNF vibrational dynamics has shown that the intensity of specific armchair and zigzag peaks strongly decreases if the largest size of the GNF is smaller than about 10 nm.

Acknowledgments

This work was partially supported by the French "Agence Nationale de la Recherche" (ANR) through Project NANOSIM_GRAPHENE (ANR-09-NANO-016). The authors would like to thank D. Van Nam and V. Hung Nguyen for useful discussions.

References

* Electronic address: `fulvio.mazzamuto@u-psud.fr`
† Present address: CEA-DIF, B.P. 12, F-91680 Bruyères-le-Châtel, France

[1] M. Yamada, Y. Yamakita, and K. Ohno, Physical Review B **77**, 054302 (2008).
[2] M. Ezawa, Physical Review B **73**, 045432 (2006).
[3] S. Cho, Y. Chen, and M. Fuhrer, Applied Physics Letters **91**, 123105 (2007).
[4] V. H. Nguyen, V. N. Do, A. Bournel, V. L. Nguyen, and P. Dollfus, Journal of Applied Physics **106**, 053710 (2009).
[5] N. Tombros, C. Jozsa, M. Popinciuc, H. Jonkman, and B. Van Wees, Nature **448**, 571 (2007).
[6] S. Ghosh, I. Calizo, D. Teweldebrhan, E. Pokatilov, D. Nika, A. Balandin, W. Bao, F. Miao, and C. Lau, Applied Physics Letters **92**, 151911 (2008).
[7] O. Yijian and G. Jing, Applied Physics Letters **94**, 263107 (2009).
[8] D. Dragoman and M. Dragoman, Applied Physics Letters **91**, 203116 (2007).
[9] A. C. Ferrari, Solid State Communications **143**, 47 (2007).
[10] F. Tuinstra and J. L. Koenig, The Journal of Chemical Physics **53**, 1126 (1970).
[11] A. C. Ferrari, Phys. Rev. Lett. **97**, 187401 (2006).
[12] L. M. Malard, M. A. Pimenta, G. Dresselhaus, and M. S. Dresselhaus, Physics Reports **473**, 51 (2009).
[13] C. Casiraghi, A. Hartschuh, H. Qian, S. Piscanec, C. Georgi, A. Fasoli, K. S. Novoselov, D. M. Basko, and A. C. Ferrari, Nano Letters **0** (2009).
[14] W. Ren, *et al.*, Physical Review B **81**, 035412 (2010).

[15] R. Gillen, M. Mohr, C. Thomsen, and J. Maultzsch, Physical Review B **80**, 155418 (2009).
[16] J. Zhou and J. Dong, Applied Physics Letters **91**, 173108 (2007).
[17] M. Vandescuren, P. Hermet, V. Meunier, L. Henrard, and P. Lambin, Physical Review B **78**, 195401 (2008).
[18] K. Ohno, Journal of Molecular Spectroscopy **72**, 238 (1978).
[19] A. Grüneis, R. Saito, T. Kimura, L. G. Canado, M. A. Pimenta, A. Jorio, A. G. Souza Filho, G. Dresselhaus, and M. S. Dresselhaus, Physical Review B **65**, 155405 (2002).
[20] L. Wirtz and A. Rubio, Solid State Communications **131**, 141 (2004).
[21] A. C. Ferrari and J. Robertson, Physical Review B **61**, 14095 (2000).
[22] A. Milani, M. Tommasini, M. Del Zoppo, C. Castiglioni, and G. Zerbi, Physical Review B **74**, 153418 (2006).
[23] L. G. Canado, M. A. Pimenta, B. R. A. Neves, M. S. S. Dantas, and A. Jorio, Physical Review Letters **93**, 247401 (2004).
[24] S. Rols, Z. Benes, E. Anglaret, J. L. Sauvajol, P. Papanek, J. E. Fischer, G. Coddens, H. Schober, and A. J. Dianoux, Physical Review Letters **85**, 5222 (2000).
[25] M. D. R. Saito, *Physical properties of carbon nanotubes* (Imperial College Press, 1998).
[26] L. A. Falkovsky, Journal of Experimental and Theoretical Physics **105** (2007).
[27] L. A. Falkovsky, Physics Letters A **372**, 5189 (2008).
[28] R. Saito, T. Takeya, T. Kimura, G. Dresselhaus, and M. S. Dresselhaus, Physical Review B **57**, 4145 (1998).
[29] M. Mohr, J. Maultzsch, E. Dobardzic, S. Reich, I. Milosevic, M. Damnjanovic, A. Bosak, M. Krisch, and C. Thomsen, Physical Review B **76**, 035439 (2007).
[30] N. Mounet and N. Marzari, Physical Review B **71**, 205214 (2005).
[31] H. Yanagisawa, T. Tanaka, Y. Ishida, M. Matsue, E. Rokuta, S. Otani, and C. Oshima, Surface and Interface Analysis **37**, 133 (2005).
[32] A. S. Barnard and I. K. Snook, The Journal of Chemical Physics **128**, 094707 (2008).